J Neuropathol Exp Neurol
Vol. 65, No. 11
November 2006
pp. 1090–1097

ORIGINAL ARTICLE

Upregulated Expression of Purinergic $P2X_7$ Receptor in Alzheimer Disease and Amyloid-β Peptide-Treated Microglia and in Peptide-Injected Rat Hippocampus

James G. McLarnon, PhD, Jae K. Ryu, MSc, Douglas G. Walker, PhD, and Hyun B. Choi, BSc

Abstract

The expression of the purinergic receptor subtype $P2X_7R$, a nonselective cationic channel activated by high levels of adenosine triphosphate (ATP), has been studied in adult microglia obtained from Alzheimer disease (AD) and nondemented (ND) brains, in fetal human microglia exposed to $A\beta_{1\text{-}42}$ peptide and in vivo in $A\beta_{1\text{-}42}$-injected rat hippocampus. Semiquantitative reverse transcriptase–polymerase chain reaction showed enhanced expression (increase of 70%) of $P2X_7R$ in AD microglia compared with ND cells (analysis of 6 AD and 8 ND cases). Immunohistochemical analysis showed prominent $P2X_7R$ expression in association with Aβ plaques and localized to HLA-DR-immunoreactive microglia. In cultured fetal human microglia, cells exposed to $A\beta_{1\text{-}42}$ (5 μM for 18 hours) had significantly elevated levels of $P2X_7R$ (by 106%) compared with untreated cells. Amplitudes of Ca^{2+} responses in these cells, induced by the selective $P2X_7R$ agonist BzATP, were increased by 145% with $A\beta_{1\text{-}42}$ pretreatment relative to control (no peptide pretreatment) and were largely blocked if the $P2X_7R$ inhibitor-oxidized ATP (oxATP) was added with peptide in pretreatment solution. In vivo, double immunostaining analysis showed considerable $P2X_7R$ colocalized with microglia after injection of $A\beta_{1\text{-}42}$ (1 nmol) into rat hippocampus. The overall results suggest roles of $P2X_7R$ in mediating microglial purinergic inflammatory responses in AD brain.

Key Words: Alzheimer disease, Amyloid-β, Calcium imaging, Immunohistochemistry, Microglia, $P2X_7$ receptor.

INTRODUCTION

Increased extracellular levels of adenosine triphosphate (ATP) are associated with cellular damage in brain pathology. Leakage of ATP from damaged cells serves as a chemotactic gradient and signal for mobilization and activation of microglia, the immune responding cells of the brain. On activation, microglia express and produce a diversity of factors, which, in assemblage, constitute an inflammatory response to help resolve the original damage. However, this response has the potential of either aiding in the promoting of cell survival to repair injury or, in extreme cases, possibly exacerbating the neuronal damage. The net outcome of the inflammatory response is likely dependent on a number of factors, including the local concentration of ATP and the duration and nature of the initial damage. Presumably, higher and chronic levels of ATP could be indicative of more severe cell damage, thus favoring a proinflammatory response from microglia.

Purinergic receptors comprise the metabotropic P2YR family and the ionotropic P2XR family (1). The P2YR are G-protein coupled to inositol triphosphate-mediated calcium (Ca^{2+}) release from endoplasmic reticulum stores. Depletion of Ca^{2+} from stores leads to a secondary entry of Ca^{2+} through store-operated channels located in plasmalemmal membrane. The P2XR family comprises $P2X_1R$-$P2X_7R$ and are directly coupled to nonselective cationic channels allowing influx of Na^+ and Ca^{2+}, efflux of K^+, and a net cell depolarization. Functional interactions between the 2 subtypes of purinergic receptors have been reported in human microglia with cell depolarization mediated by ATP binding to a subtype P2XR (not $P2X_7R$) acting to inhibit influx of Ca^{2+} through store-operated channels subsequent to ATP activation of P2YR (2, 3).

A particularly unique member of P2XR is $P2X_7R$ that, when activated by ATP binding, forms a large pore allowing entry of large hydrophilic cationic molecules. The results from a number of studies have suggested that extracellular levels of ATP in excess of 1 mM are generally required for activation of $P2X_7R$ (3–5). The high concentration of ATP required to open channels could indicate that functional responses mediated by $P2X_7R$ are associated with ongoing cellular damage and chronic brain inflammation. In this regard, activation of $P2X_7R$ in microglia has been correlated with production of the proinflammatory cytokines tumor necrosis factor-α (TNF-α) (5) and interleukin-1β (IL-1β) (6, 7) and also with cell apoptosis (8, 9). Recent work has documented roles of $P2X_7R$ in the microglial production of superoxide and that expression of the receptor is upregulated in a transgenic mouse model of Alzheimer disease (AD) (10).

From the Department of Anesthesiology, Pharmacology and Therapeutics (JGC, JKR, HBC), University of British Columbia, Vancouver BC, Canada; and the Laboratory of Neuroinflammation (DGW), Sun Health Research Institute, Sun City, Arizona.

Send correspondence and reprint requests to: James G. McLarnon, PhD, Department of Anesthesiology, Pharmacology and Therapeutics, University of British Columbia, 2176 Health Sciences Mall, Vancouver, BC, V6T 1Z3, Canada; E-mail: mclarnon@interchange.ubc.ca

This work was supported by grants from Alzheimer's Society of Canada and Alzheimer's Association USA (JGM) and grant AG 18345 from National Institute of Health (DGW).

In this study, we have compared the expression of $P2X_7R$ in microglia obtained from neuropathologically assessed AD brain (6 cases) and nondemented (ND, 8 cases). In addition, we have compared expression of this subtype ionotropic receptor between amyloid-β peptide ($A\beta_{1-42}$)-treated and untreated cultured fetal human microglia. Calcium responses induced by the $P2X_7R$ ligand BzATP have also been determined in untreated microglia or cells previously exposed to $A\beta_{1-42}$. Finally, we have measured expression of $P2X_7R$ in $A\beta_{1-42}$-injected rat hippocampus.

MATERIALS AND METHODS

Adult Human Microglia

Adult brains were obtained postmortem from individuals who had signed informed consent forms for brain donation to the Brain Donation Program of the Sun Health Research Institute (11). Neuropathologic analysis was carried out on all donated brains with diagnosis of AD using criteria established in the Consortium to Establish a Registry for Alzheimer's disease. Nondemented brain was characterized by plaque and tangle scores inconsistent with AD and a lack of clinical dementia in donor individuals. Postmortem intervals for isolation of ND and AD brains were 2.8 ± 0.5 hours (n = 8 cases) and 2.1 ± 0.2 hours (n = 6 cases), respectively; these times were not significantly different.

Cultured adult human microglia were obtained from brain tissue following published procedures (12,13). As noted, isolation of ND and AD brains were carried out within 3 hours postmortem. Immediately after the isolation procedure, brain tissue was enzymatically dissociated and microglia were harvested and placed under culture conditions following standard protocols (14). Briefly, microglia were separated from other glial cells by differential adherence and maintained in Dulbecco's modified Eagle medium (DMEM) with high glucose (5 mg/mL) containing 10% fetal bovine serum (Hyclone, Salt Lake City, UT) and 50 μg/mL gentamicin. Microglia were used in experiments after 10 to 14 days in culture and cell purity was assessed by using immunocytochemistry with antibodies to CD11b (American Type Culture Collection [ATCC], Manassas, VA) to class II major histocompatibility antigen (HLA-DR) (1:800; ICN Pharmaceuticals, Irvine, CA) and to CD68 (1:1000; Accurate Chemical and Scientific Corp. Westbury, NY). Antibody to glial fibrillary acidic protein (GFAP, 1:5,000; Dako, Raleigh, NC) was used to measure astrocyte contamination. Immunocytochemical results showed purity of microglia was in excess of 98%.

Fetal Human Microglia

Fetal cells were obtained from embryonic tissue after legalized therapeutic abortions as certified by the Ethics Committee of the University of British Columbia. The overall procedures of isolation and identification of microglia have been previously described (15). In brief, brain tissues of 12 to 18 weeks' gestation were incubated in phosphate-buffered saline (PBS) with 0.25% trypsin and DNase I (40 μg/mL) for 30 minutes at 37°C. Cells were separated into single cells by repeated gentle pipetting. Dissociated cells were then maintained in T75 flasks in DMEM containing 5% horse serum, 5 mg/mL glucose, 20 μg/mL gentamicin, and 2.5 μg/mL amphotericin B. Floating microglia in a medium were harvested after 7 to 10 days and subsequently plated on 6-well multiplates for reverse transcriptase–polymerase chain reaction. CD11b and ricinus communis agglutinin, specific markers for microglia, were used to confirm purity of the cultures exceeded 98%.

Preparation and In Vitro and In Vivo Application of Amyloid-β Peptide

Full-length peptide ($A\beta_{1-42}$) was obtained from California Peptides (Napa, CA). Aggregated peptide for microglial stimulation was prepared following procedures outlined previously (16). Aggregated $A\beta_{1-42}$ was dissolved in 35% acetonitrile (Sigma, St. Louis, MO) and diluted to 1.5 mM with sterile water. Sequential additions of PBS with vortexing of solutions were used to prepare a peptide concentration of 0.5 mM. A final step was to maintain peptide solution at 37°C for 18 hours to enhance fibril formation and aggregation before storage at –20°C. Reverse peptide $A\beta_{42-1}$ (California Peptides) was also used in some experiments with preparation following that described for $A\beta_{1-42}$.

Forward and reverse peptides were applied in vitro to cultured fetal human microglia. The studies used 18-hour exposure of cells to 5 μM concentrations of peptides. A similar treatment protocol has been applied to human microglia in testing for cellular expression and production of a spectrum of inflammatory mediators (17).

For in vivo studies, male Sprague-Dawley rats (250–280 g; Charles River Laboratories, St. Constant, Quebec, Canada) were anesthetized with intraperitoneal injection of a mixture of ketamine hydrochloride (72 mg/kg; Bimeda-MTC, Cambridge, Ontario, Canada) and xylazine hydrochloride (9 mg/kg; Bayer Inc., Etobicoke, Ontario, Canada) and then mounted in a stereotaxic apparatus (Kopf Instruments, Tujunga, CA). $A\beta_{1-42}$ or $A\beta_{42-1}$ (1 nmol in 2 μL) or PBS was slowly injected (0.2 μL/minute) into the superior blade of dentate gyrus of the hippocampus (anteroposterior: −3.6 mm; mediolateral: −1.8 mm; dorsoventral: −3.2 mm) with a 10-μL Hamilton syringe. All animal procedures were approved by the University of British Columbia Animal Care Ethics Committee adhering to guidelines of the Canadian Council on Animal Care.

Reverse Transcriptase–Polymerase Chain Reaction Analysis

Fetal human microglia were plated on 6-well multiplates and were exposed to $A\beta_{1-42}$ or reverse peptide $A\beta_{42-1}$ (applications at 5 μM for 18 hours) or PBS. Adult microglia from ND individuals and patients with AD were also used for reverse transcriptase–polymerase chain reaction (RT-PCR) experiments. Isolation of RNAs was performed using TRIzol (Gibco-BRL, Gaithersburg, MD) and DNA contamination was eliminated using DNase. Complementary DNA synthesis was carried out using M-MLV reverse transcriptase (Gibco-BRL).

For in vivo RT-PCR analysis, animals were deeply anesthetized and killed by decapitation at 3 days postinjection of $A\beta_{1-42}$, reverse peptide $A\beta_{42-1}$, or PBS. After removal of brains, tissue samples from hippocampus were prepared and

frozen in liquid nitrogen. Total RNA was extracted using TRIzol subjected to DNase I treatment and complementary DNA synthesis carried out using M-MLV reverse transcriptase. M-MLV was omitted as a negative control. PCR primer sequences with expected product size are as follows: human $P2X_7R$ sense 5′-ACAATGTTGAGAAACGGAC-TCTGA-3′ and human $P2X_7R$ antisense 5′-CCGGCT-GTTGGTGGAATCCACATC-3′ (728 bp); rat $P2X_7R$ sense 5′-AGGAGCCCCTTATCAGCTCT-3′ and rat $P2X_7R$ antisense 5′-CATTGGTGTACTTGTCGTCC-3′ (692 bp); human GAPDH sense 5′-CCATGTTCGTCATGGGTGT-GAACCA-3′ and human GAPDH antisense 5′-GCCAGTA-GAGGCAGGGATGATGTTC-3′ (251 bp); and rat β-actin sense 5′-GTGGGGCGCCCCAGGCACCA-3′ and rat β-actin antisense 5′-GTCCTTAATGTCACGCACGATTTC-3′ (526 bp).

PCR conditions were as follows: initial denaturation at 95°C for 6 minutes followed by 35 cycles of denaturation at 95°C for 45 seconds, annealing at 60°C for 1 minute, and extension at 72°C for 1 minute. A final extension was carried out at 72°C for 10 minutes. The amplified PCR products were identified using 1.5% agarose gels containing ethidium bromide and visualized under ultraviolet light. The intensities of each band were measured by densitometry using the NIH Image J 1.24 software (National Institutes of Health, Bethesda, MD) and expressed as relative mRNA levels ($P2X_7R$ mRNA levels normalized to GAPDH or β-actin) (17). Glyceraldehyde-3-phosphate dehydrogenase (GAPDH) and β-actin were used as reaction standards for human and rat, respectively.

Calcium Sensitive Fluorescence Microscopy

The procedures used for measurement of intracellular Ca^{2+} $[Ca^{2+}]_i$ have been documented (18). In brief, microglia were incubated with fura-2/AM (acetoxymethyl ester, at 1 μM; Molecular Probes, Eugene, OR) plus pluronic acid (at 1 μM) in normal physiological saline solution (PSS) for 30 minutes. PSS contained (in mM): NaCl (126), KCl (5), $MgCl_2$ (1.2), HEPES (10), D-glucose (10), and $CaCl_2$ (1); pH of 7.4. All reagents were obtained from Sigma-Aldrich (St. Louis, MO). After a 20-minute wash in dye-free PSS, coverslips were placed on the stage of a Zeiss Axiovert inverted microscope using a ×40 quartz objective lens. Cells were exposed to alternating excitation wavelengths of 340 nm and 380 nm at 6-second intervals and emission light was passed through a 510-nm filter. An imaging system (Empix Imaging, Mississauga, ON, Canada) was used to record fluorescence ratios using a CCD camera (Retiga 1300i, Burnaby, BC, Canada). Results are presented as ratios F340/F380 versus time with all experiments done at room temperature (RT, 20–22°C).

Immunohistochemistry of Human Brain

All human samples were obtained from the Brain Bank at the Sun Health Research Institute (Sun City, AZ). The procedures for immunohistochemistry in human tissues were conducted according to previously described methods (19). In brief, immunohistochemistry for localization of antigens was carried out on 20-μm free-floating tissue sections using single and 2 color procedures as described (19). The antibody to $P2X_7R$ (Alomone Laboratory, Jerusalem, Israel) was used at 1:250 first and detected with nickel enhanced diaminobenzidine substrate (19) to give a blue reaction product; sections were subsequently reacted with 3D6 (antibody to N-terminal Aβ peptide, 1:3,000; provided by Elan Pharmaceuticals, South San Francisco, CA) or with LN3 (1:500; MP Biochemicals, OH), and then reacted with DAB substrate without nickel to give a brown reaction product.

Immunohistochemical Analysis of Rat Brain

Animals were deeply anesthetized and then transcardially perfused with heparinized cold saline followed by 4% paraformaldehyde in 0.1 M phosphate buffer (0.1 M PB, pH 7.4). The brains were removed from the skull and postfixed in the same fixative solution overnight and then placed in 30% sucrose for cryoprotection. The brains were then frozen in powdered dry ice and stored at –70°C. Coronal sections throughout the hippocampus were cut at 40-μm intervals on a cryostat. The sections were stored in cryoprotectant solution. For $P2X_7R$ expression, free-floating sections were permeabilized with 0.2% Triton X-100 and 0.5% BSA in 0.1 M PBS for 30 minutes and then incubated overnight at 4°C with primary antibody against $P2X_7R$ (1:200; Alomone Laboratory). Sections were then sequentially incubated with Alexa Fluor-conjugated 488 anti-rabbit IgG (1:100; Molecular Probes) at RT for 2 hours in the dark. For double immunofluorescence immunohistochemistry, free-floating sections were incubated overnight at 4°C with a mixture of 2 primary antibodies: $P2X_7R$ in combination with Aβ (1:500; Abcam, Cambridge, MA), OX-42 (1:200; Serotec, Oxford, UK), or GFAP (1:500; Sigma). Sections were then incubated in a mixture of Alexa Fluor-conjugated 488 anti-rabbit IgG (1:100; Molecular Probes) and Alexa Fluor 594-conjugated anti-mouse IgG (1:100; Molecular Probes) at RT for 2 hours in the dark. Stained sections were examined under a Zeiss Axioplan 2 fluorescent microscope and images were acquired with a DVC camera (Diagnostic Instruments, Sterling Heights, MI). For quantification of $P2X_7R$ immunoreactivity, mean gray level of immunoreactivity was measured and quantified using Northern Eclipse software (Empix Imaging, Mississauga, ON, Canada) (20). All quantitative analyses were carried out in a blinded manner.

Statistical Analysis

All results are presented as mean ± standard error of mean. Statistical significance ($p < 0.05$) was evaluated using Student *t*-test or one-way analysis of variance followed by Student-Newman-Keuls multiple comparison test when applicable (GraphPad Prism 3.0; San Diego, CA).

RESULTS

$P2X_7R$ Expression in Microglia from Patients With Alzheimer Disease and Nondemented Individuals

RT-PCR was carried out for expression of $P2X_7R$ in microglia obtained from 14 individuals. Of these, 6 were confirmed as AD and 8 showed no diagnosis for AD symptoms and were confirmed as ND (see "Materials and

Methods"). Representative band intensities for microglial $P2X_7R$ expressions are shown for one ND case and one AD case (Fig. 1A); also shown is GAPDH as a reaction standard. In general, microglia obtained from ND individuals showed weak band intensity for $P2X_7R$, indicating a low constitutive expression for this subtype of purinergic receptor. However, microglia from all AD cases showed strong expressions for $P2X_7R$.

The results from semiquantitative analysis of band intensities are presented in Figure 1B showing relative mRNA levels of $P2X_7R$ in AD and ND microglia. Overall, the expression of $P2X_7R$ was increased by 70% in AD microglia (n = 6 cases) compared with ND cells (n = 8 cases). Immunohistochemical procedures were also applied to examine expression of $P2X_7R$ protein in AD brain sections (Fig. 2). $P2X_7R$ immunoreactivity was observed throughout sections (Fig. 2A, blue staining) but was prominently expressed in association with Aβ plaques (Fig 2A, brown staining). Weak $P2X_7R$ immunoreactivity was seen on cells with morphologic appearance of microglia throughout the tissue sections in both white and grey matter. Using an antibody to HLA-DR to identify microglia, stronger $P2X_7R$ staining correlated with stronger HLA-DR immunoreactivity (Fig. 2B). Staining for $P2X_7R$ was only observed on cells that had immunoreactivity for HLA-DR and had the morphology of microglia. Little or no evidence for $P2X_7R$ immunoreactivity was found in ND brain sections (data not shown).

$P2X_7R$ Expression in $A\beta_{1\text{-}42}$-Treated and Untreated Human Microglia

AD brains are characterized by senile plaques of fibrillar $A\beta_{1\text{-}42}$ peptide and neurofibrillary tangles. We next examined the effects of exposure of cultured fetal human microglia to $A\beta_{1\text{-}42}$ (at 5 μM for 18 hours); 2 controls were used with one group treated with PBS and another group treated with reverse peptide $A\beta_{42\text{-}1}$ (at 5 μM for 18 hours). The representative results from a single RT-PCR assay for $P2X_7R$ are presented in Figure 3A. Human microglia exposed to PBS or to $A\beta_{42\text{-}1}$ exhibited a low level of band intensity for $P2X_7R$, whereas $A\beta_{1\text{-}42}$-treated cells showed a robust expression for this subtype purinergic receptor (Fig. 3A). GAPDH was used as a reaction standard (Fig. 3A, lower panel).

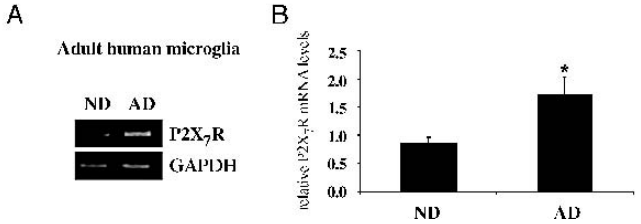

FIGURE 1. Expression of $P2X_7R$ in microglia isolated from nondemented (ND) and Alzheimer disease (AD) brain. **(A)** Representative reverse transcriptase–polymerase chain reaction for levels of $P2X_7R$ in adult ND and AD microglia. Glyceraldehyde-3-phosphate dehydrogenase was used as a reaction standard. **(B)** Relative mRNA levels for $P2X_7R$ from analysis of brains from 8 ND and 6 AD individuals. *, $p < 0.05$ compared with ND.

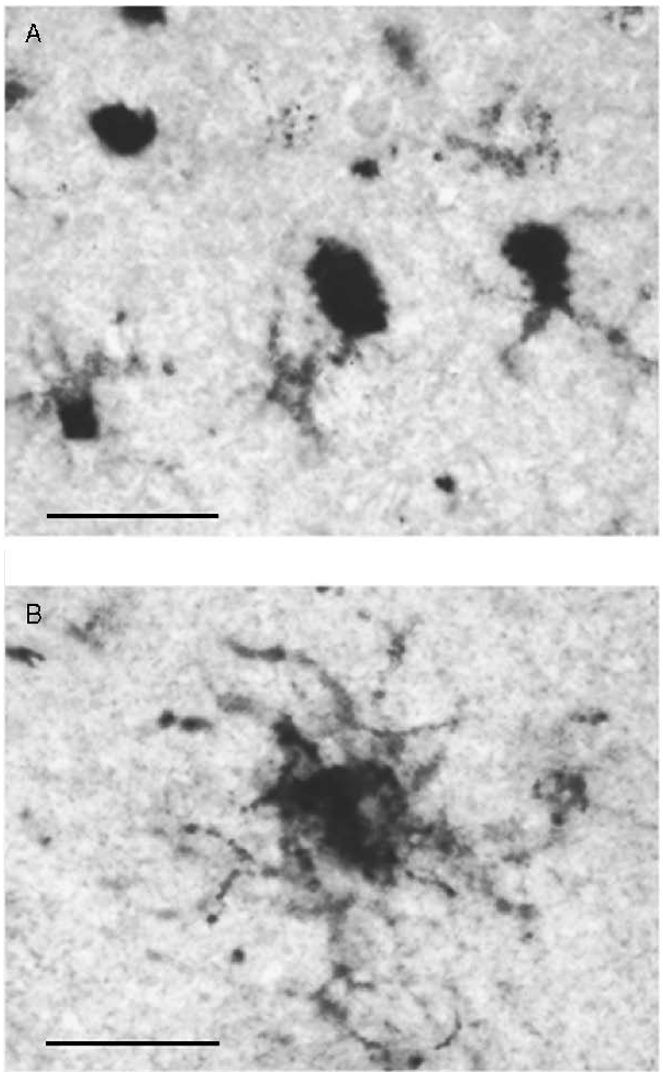

FIGURE 2. Photomicrographs showing $P2X_7R$-immunoreactive cells around Aβ plaques and colocalization of $P2X_7R$ with HLA-DR+ microglia. **(A)** Representative immunoreactivity for $P2X_7R$ (blue) in the vicinity of Aβ-immunoreactive plaques (brown). The morphologies of stained cells are consistent with microglia. Scale bar = 30 μm. **(B)** Example of $P2X_7R$ immunoreactivity (blue) associated with HLA-DR+ microglia (brown). Scale bar = 10 μm.

The quantification of results is presented in Figure 3B. Treatment of human microglia with $A\beta_{1\text{-}42}$ peptide (n = 6) significantly increased $P2X_7R$ expression (by 106%) relative to PBS control (n = 6) and by 76 % compared with reverse peptide (n = 5).

Functional Responses of $P2X_7R$ in $A\beta_{1\text{-}42}$-Pretreated and Untreated Human Microglia

It was of interest to determine if $P2X_7R$-mediated responses in fetal human microglia were modulated by cellular exposure to $A\beta_{1\text{-}42}$. This point was studied using the

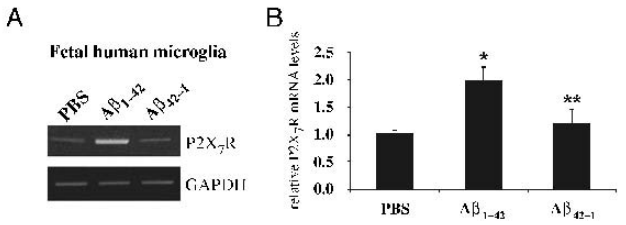

FIGURE 3. Expression of $P2X_7R$ in $A\beta_{1\text{-}42}$ stimulated fetal human microglia. **(A)** Representative expression of $P2X_7R$ with microglia exposed to phosphate-buffered saline, $A\beta_{1\text{-}42}$, and $A\beta_{42\text{-}1}$ with glyceraldehyde-3-phosphate dehydrogenase used as a reaction standard. (**B**) Relative expression of $P2X_7R$ for the different treatments (n = 6 for phosphate-buffered saline and $A\beta_{1\text{-}42}$ and n = 5 for $A\beta_{42\text{-}1}$). *, $p < 0.05$ compared with the phosphate-buffered saline-treated group. **, $p < 0.05$ compared with the $A\beta_{1\text{-}42}$-treated group.

selective $P2X_7R$ agonist BzATP to elicit entry of Ca^{2+} through the nonselective cationic channel associated with this receptor. Human microglial cells were placed in culture medium and grouped as control (no exposure to $A\beta_{1\text{-}42}$ peptide), $A\beta_{1\text{-}42}$-treated (exposure to 5 μM peptide for 18 hours), and $A\beta_{1\text{-}42}$-treated in the presence of oxATP (a specific inhibitor of $P2X_7R$). In the latter group, oxATP (at 300 μM) was applied 2 hours before, and for the duration of, peptide application.

Representative results are presented in Figure 4A. In microglia pretreated with $A\beta_{1\text{-}42}$, BzATP (at 300 μM) caused a large increase in $[Ca^{2+}]_i$ (measured by the change in wavelength ratio, 340/380 nm), which continued to grow in amplitude to a plateau level at 10 minutes postapplication of the purinergic ligand (n = 32 cells). In the presence of oxATP, the response elicited by BzATP from peptide-treated cells was markedly reduced (n = 18 cells). BzATP evoked a small increase in $[Ca^{2+}]_i$ in untreated microglia (control, n = 28 cells). oxATP was effective in abolishing control responses (control + oxATP; n = 27 cells).

Quantification of BzATP-induced Ca^{2+} responses with the different treatments was determined by measurement of the peak amplitudes of $[Ca^{2+}]_i$ with respect to baseline levels. With $A\beta_{1\text{-}42}$ pretreatment (n = 5 experiments; 95 cells), response amplitudes were increased by 145% relative to control (n = 4 experiments; 87 cells) (Fig. 4B). With oxATP included together with $A\beta_{1\text{-}42}$ in the pretreatment solution (n = 4 experiments; 82 cells), Ca^{2+} responses were decreased by 86% relative to peptide alone. oxATP application to control completely blocked BzATP responses (n = 4 experiments, 76 cells).

$P2X_7R$ Expression in Rat Hippocampus

We next investigated the expression of $P2X_7R$ in rat hippocampus for 3 different groups of animals: those receiving intrahippocampal injections of PBS, $A\beta_{1\text{-}42}$, or $A\beta_{42\text{-}1}$. Peptides were injected at 1 nmol with all analyses carried out at 3 days postinjection. Representative RT-PCR is presented in Figure 5A showing a low basal level of $P2X_7R$ after PBS injection. A considerably enhanced expression of the purinergic receptor was observed with

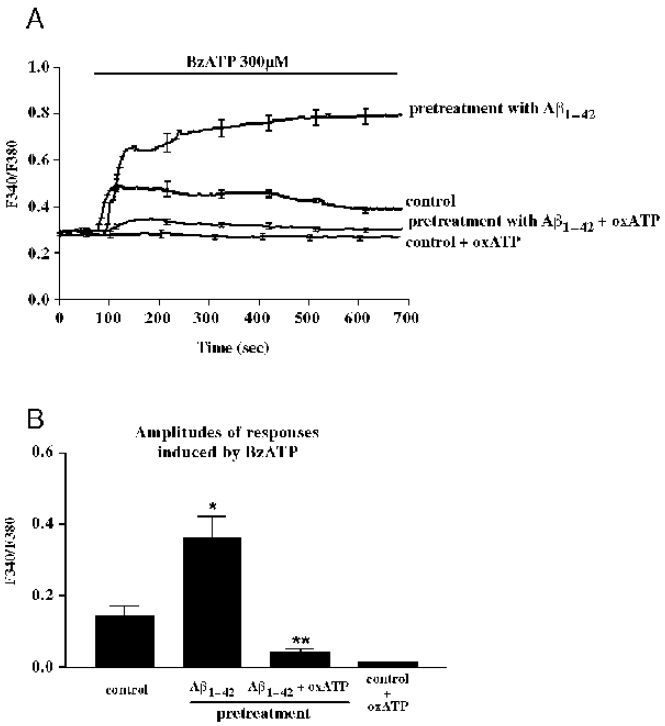

FIGURE 4. Changes in $[Ca^{2+}]_i$ induced by the $P2X_7R$ agonist BzATP. **(A)** Application of BzATP (at 300 μM) was used to increase intracellular Ca^{2+} (measured by changes in F340/F380). Representative traces show (top to bottom) responses with $A\beta_{1\text{-}42}$ pretreatment (5 μM for 18 hours, n = 32 cells), control (no peptide pretreatment, n = 28 cells), peptide pretreatment in the presence of oxATP (300 μM and added 2 hours before peptide [n = 18 cells]) and oxATP pretreatment alone (n = 27 cells). **(B)** Amplitudes of responses induced by BzATP for the different treatments (4–5 independent experiments for each groups). *, $p < 0.05$ compared with control. **, $p < 0.05$ compared with the $A\beta_{1\text{-}42}$-pretreated group.

injection of $A\beta_{1\text{-}42}$, whereas $A\beta_{42\text{-}1}$ was associated with a low level of $P2X_7R$ (Fig. 5A). β-actin was used as a reaction standard (Fig. 5A, lower panel). Semiquantitative results for the 3 groups of injected animals (n = 3 for each) are shown

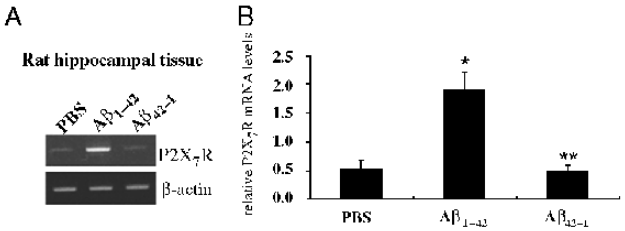

FIGURE 5. In vivo expression of $P2X_7R$ in rat hippocampus. **(A)** Representative reverse transcriptase–polymerase chain reaction for $P2X_7R$ in rat hippocampus at 3 days postinjection with phosphate-buffered saline, $A\beta_{1\text{-}42}$, or $A\beta_{42\text{-}1}$ (peptides at 1 nmol). **(B)** Relative mRNA levels for $P2X_7R$ with the different treatments (n = 3 for each). *, $p < 0.05$ compared with the phosphate-buffered saline-injected group. **, $p < 0.05$ compared with the $A\beta_{1\text{-}42}$-injected group.

in Figure 5B. The expression of $P2X_7R$ was increased 4-fold in $A\beta_{1\text{-}42}$-injected, relative to PBS or reverse peptide-injected, rat hippocampus.

We also used immunohistochemical procedures to investigate expression of $P2X_7R$ protein in the dentate gyrus (Fig. 6A, top left panel, portion of superior blade denoted by dotted line). Within the superior blade region, minimal $P2X_7R$ immunoreactivity was evident at 3 days after injection of PBS (Fig. 6A, top right panel). However, immunoreactivity for $P2X_7R$ was markedly elevated in $A\beta_{1\text{-}42}$-but not $A\beta_{42\text{-}1}$-injected animals (Fig. 6A, bottom panels). Quantification of $P2X_7R$ immunoreactivity demonstrates the extent of $P2X_7R$ immunoreactivity induced with $A\beta_{1\text{-}42}$ injection compared with PBS or $A\beta_{42\text{-}1}$-injected animals (Fig. 6B, n = 4 for each group).

A representative double immunostaining result is presented showing extensive areas of $P2X_7R$ immunoreactivity in proximity to $A\beta_{1\text{-}42}$ deposits (Fig. 6C, left panel). The morphology of cells expressing $P2X_7R$ was consistent with microglia. We next used double immunostaining to enable identification of the specific cells that were associated with expression of $P2X_7R$. Representative double immunofluorescent staining is presented in Figure 6C for $P2X_7R$ with OX-42 (microglial marker, middle panel) or GFAP (astrocyte marker, right panel). The results showed colocalization of $P2X_7R$ and OX-42+ microglia within the hippocampus after $A\beta_{1\text{-}42}$ injection (Fig. 6C, middle panel). Only a small subset of GFAP+ astrocytes was associated with $P2X_7R$ (Fig. 6C, right panel). No colocalization of the purinergic receptor with NeuN+ neurons was observed (data not shown).

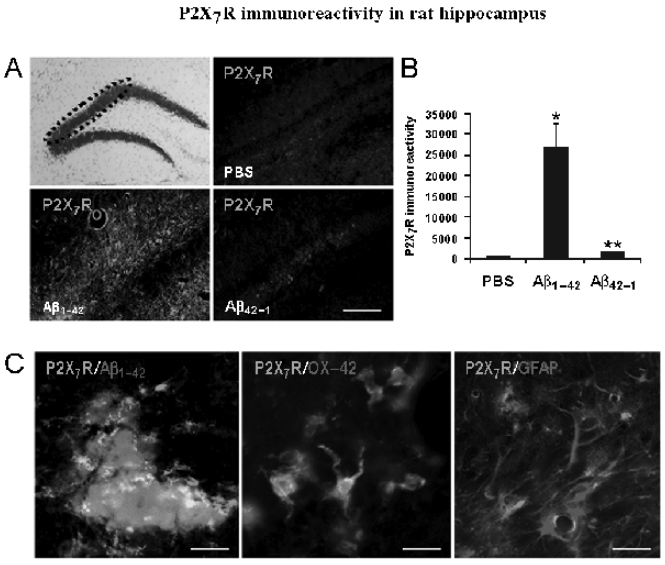

FIGURE 6. Single and double immunostaining for $P2X_7R$ in rat hippocampus. (**[A]**, upper left panel): A portion of the superior blade is indicated by the dotted region. The other panels of Figure A show expression of $P2X_7R$ in the indicated region at 3 days after injections of phosphate-buffered saline (upper right panel), $A\beta_{1\text{-}42}$ (lower left panel), and $A\beta_{42\text{-}1}$ (lower right panel). Scale bar = 150 μm. **(B)** Quantification of $P2X_7R$ immunoreactivity for the different treatments (n = 4 for each). *, $p < 0.05$ compared with the phosphate-buffered saline-injected group. **, $p < 0.05$ compared with the $A\beta_{1\text{-}42}$-injected group. **(C)** Representative double staining for $P2X_7R$ (green marker) with $A\beta_{1\text{-}42}$ peptide (red marker, left panel), microglia (red marker, middle panel), or astrocytes (red marker, right panel). Scale bars = 30 μm.

DISCUSSION

An important and novel finding from this study is that expression of $P2X_7R$ is upregulated in microglia in AD, compared with levels in ND, brain. We also report that fetal human microglia stimulated with $A\beta_{1\text{-}42}$ peptide exhibit considerably elevated expressions of $P2X_7R$ relative to control (untreated cells and $A\beta_{42\text{-}1}$) and show marked increases in $[Ca^{2+}]_i$ in response to a $P2X_7R$ agonist after exposure to peptide. In addition, $P2X_7R$ was markedly upregulated in $A\beta_{1\text{-}42}$-injected compared with PBS or $A\beta_{42\text{-}1}$-injected rat hippocampus.

Microglia obtained from ND brain show a low level of expression for $P2X_7R$; however, considerable upregulation of the purinergic receptor was evident in AD microglia (Fig. 1A). Semiquantitative RT-PCR (Fig. 1B) indicated an approximate 2-fold increase in mRNA levels in AD, relative to ND, microglia. The constitutive expression of $P2X_7R$ in ND microglia could be associated with a relatively low basal activation of cells. Microglia in ND brain exhibit a predominantly ramified morphology; however, some ameboid-shaped cells were observed (13). Cells obtained from AD individuals present a primary ameboid morphology (13). The respective ramified and ameboid morphologies are commonly associated with resting and activated states of microglia (14).

Cultured fetal human microglia exposed to $A\beta_{1\text{-}42}$ (5 μM for 18 hours) exhibited a marked increase in the expression of $P2X_7R$ compared with PBS or reverse peptide-treated cells. Relative mRNA levels were increased in excess of 2-fold in microglia exposed to $A\beta_{1\text{-}42}$ compared with PBS. Together with the results from Figure 1, our findings suggest low constitutive expressions of the purinergic receptor in unstimulated microglia. Functionally, microglia pretreated with $A\beta_{1\text{-}42}$ showed increased amplitude of $[Ca^{2+}]_i$ compared with controls when stimulated with the $P2X_7R$ agonist BzATP. In the presence of oxATP, the BzATP-induced increase in $[Ca^{2+}]_i$ was largely attenuated. These results would be consistent with a functional role for $P2X_7R$ in mediating Ca^{2+}-dependent microglial inflammatory responses under conditions relevant to AD brain. A small increase of $[Ca^{2+}]_i$ in controls was found with BzATP application; this result is consistent with RT-PCR data that showed a low basal expression of $P2X_7R$ in unstimulated cells. The effect of oxATP treatment in controls to abolish the BzATP response suggests the response is entirely attributable to activation of $P2X_7R$. Interestingly, recent work from this laboratory (13) has reported dysfunctional handling of Ca^{2+} in AD microglia (compared with ND cells) and in $A\beta_{1\text{-}42}$-treated fetal human microglia (compared with untreated cells). The altered Ca^{2+} mobilization included smaller amplitudes of ATP-induced responses for both AD

microglia and peptide-treated cells. These responses were attributed to release of Ca^{2+} from endoplasmic reticulum stores subsequent to ATP binding to P2Y subtype receptors. An important point is that these experiments used ATP at 100 μM, a level insufficient to activate $P2X_7R$ in human microglia (3).

Expression of $P2X_7R$ was markedly upregulated in $A\beta_{1\text{-}42}$-injected rat hippocampus compared with PBS or reverse peptide-injected brains. Double immunostaining procedures showed microglia were the primary cell type expressing $P2X_7R$. A small degree of $P2X_7R$ immunoreactivity was associated with astrocytes, whereas neurons exhibited no expression for the purinergic receptor. Although intrahippocampal injection of $A\beta_{1\text{-}42}$ represents a simplified model of AD brain, the in vivo results support roles for $P2X_7R$ in mediating microglial responses to peptide stimulation.

At present, the mechanisms underlying stimulus-induced upregulation in expressions of $P2X_7R$ are not known (21). A critical point in the function of $P2X_7R$ is that the receptor ion channel complex is only operational with high levels of extracellular ATP, generally in excess of 1 mM (3, 22, 23). This would suggest activation of $P2X_7R$ is associated with pathologic conditions associated with elevated ATP levels such as could occur with damaged neurons (24) or with chronically activated glia (25, 26). It is known that ATP can enhance $P2X_7R$-mediated responses in microglia and other inflammatory cells (27). In terms of the present results, enhanced expression of $P2X_7R$ in AD microglia or in vivo in peptide-injected brain could be the result of ATP released from cell injury or stimulated glia in the tissue.

Our findings with $A\beta_{1\text{-}42}$ stimulation of fetal human microglia could suggest an autocrine signaling role for ATP in a manner similar to that reported for lipopolysaccharide (LPS)-stimulated microglia (28). We also found that fetal human microglia treated with the LPS exhibit increased expressions of $P2X_7R$ (data not shown). This result could be consistent with a common activating factor such as ATP in the induction of $P2X_7R$ in microglia stimulated by $A\beta_{1\text{-}42}$ or LPS. Interestingly, coculture studies have found activated astrocytes release ATP, which in turn mediated activation of $P2X_7R$ in microglia (29). Our results do not exclude the possibility that $A\beta_{1\text{-}42}$ induces expression of $P2X_7R$ by means other than elevating levels of ATP. For example, IL-1β is reported to transiently enhance the expression of $P2X_7R$ in glia (30). Overall, multiple factors may engage in regulating $P2X_7R$, including elevated levels of extracellular ATP from damaged cells, ATP arising from paracrine sources, and the presence of proinflammatory cytokines. Because one downstream effect of $P2X_7R$ activation is cell apoptosis (28, 31), regulation of this subtype of purinergic receptor is likely under strict control.

It is important to note that $P2X_7R$-mediated microglial activation can influence the inflammatory environment in the pathogenesis of AD. Activation of the $P2X_7R$ has been shown to modulate the production of proinflammatory cytokines from $A\beta_{1\text{-}42}$ or LPS-stimulated human microglia and macrophages (26). The $P2X_7R$ ligand BzATP enhanced secretion of IL-1β with both peptide and LPS stimulation but TNF-α was only increased with the latter stimulus. Much of the deleterious effects mediated by $P2X_7R$ responses in microglia are the result of potent neurotoxic factors produced by $P2X_7R$-dependent pathways. Previous work has reported enhancement of $P2X_7R$ activation leads to increased production of proinflammatory cytokines (26, 32), superoxide anion (10), excitatory amino acids (33), and matrix metalloproteinases (34). All of these factors have been implicated in causing neuronal damage in the AD brain (35). It is possible that enhanced $P2X_7R$ expression could contribute to the increased levels of inflammatory factors such as TNF-α, IL-1β, and iNOS measured in AD compared with ND brains (36).

Overall, our results suggest the involvement of $P2X_7R$ in mediating inflammatory responses in AD brain. However, a proviso is that although $P2X_7R$ expression in microglia is enhanced in the AD brain or by exposure to $A\beta_{1\text{-}42}$, elevated ATP concentrations in excess of 1 mM may be required for activation of this receptor (3, 5). Such high levels of ATP would likely be associated with a localized environment of cellular damage and chronically activated glia responding to a brain insult such as deposits of amyloid peptide. An important question for future study is whether animal models of AD show sustained upregulation of $P2X_7R$ with long-duration applications of low (nM) levels of $A\beta_{1\text{-}42}$ peptide.

REFERENCES

1. Burnstock G. P2 purinoceptors: Historical perspective and classification. Ciba Found Symp 1996;198:1–28
2. Wang X, Kim SU, van Breemen C, et al. Activation of purinergic P2X receptors inhibits P2Y-mediated Ca^{2+} influx in human microglia. Cell Calcium 2000;27:205–12
3. McLarnon JG. Purinergic mediated changes in Ca^{2+} mobilization and functional responses in microglia: Effects of low levels of ATP. J Neurosci Res 2005;81:349–56
4. Moller T. Calcium signaling in microglial cells. Glia 2002;40:184–94
5. Hide I, Tanaka M, Inoue A, et al. Extracellular ATP triggers tumor necrosis factor-alpha release from rat microglia. J Neurochem 2000;75: 965–72
6. Ferrari D, Chiozzi P, Simonetta F, et al. Purinergic modulation of interleukin-1β release from microglial cells stimulated with bacterial endotoxin. J Exp Med 1997;185:579–82
7. Sanz JM, Di Virgilio F. Kinetics and mechanism of ATP-dependent IL-1 beta release from microglial cells. J Immunol 2000;164:4893–98
8. Ferrari D, Los M, Bauer MK, et al. P2Z purinoreceptor ligation induces activation of caspases with distinct roles in apoptotic and necrotic alterations of cell death. FEBS Lett 1999;447:71–75
9. Brough D, LeFeuvre RA, Iwakura Y, et al. Purinergic ($P2X_7$) receptor activation of microglia induces cell death via an interleukin-1-independent mechanism. Mol Cell Neurosci 2002;19:272–80
10. Parvathenani LK, Tertyshnikova S, Greco CR, et al. $P2X_7$ mediates superoxide production in primary microglia and is up-regulated in a transgenic mouse model of Alzheimer's disease. J Biol Chem 2003;278: 13309–17
11. Lue LF, Kuo YM, Roher AE, et al. Soluble amyloid beta peptide concentration as a predictor of synaptic change in Alzheimer's disease. Am J Pathol 1999;155:853–62
12. Lue LF, Brachova L, Walker DG, et al. Characterization of glial cultures from rapid autopsies of Alzheimer's and control patients. Neurobiol Aging 1996;17:421–29
13. McLarnon JG, Choi HB, Lue LF, et al. Perturbations in calcium-mediated signal transduction in microglia from Alzheimer's disease patients. J Neurosci Res 2005;81:426–35

14. Walker DG, Kim SU, McGeer PL. Complement and cytokine gene expression in cultured microglia derived from post-mortem brains. J Neurosci Res 1995;40:478–93
15. Satoh JI, Lee YB, Kim SU. T cell co-stimulatory molecules B7-1 (CD80) and B7-2 (CD86) are expressed in human microglia but not in astrocytes in culture. Brain Res 1995;704:92–96
16. Webster S, Bradt B, Rogers J, et al. Aggregation state-dependent activation of the classical complement pathway by the amyloid beta peptide. J Neurochem 1997;69:388–98
17. Franciosi S, Choi HB, Kim SU, et al. IL-8 enhancement of amyloid-beta ($A\beta_{1-42}$)-induced expression and production of pro-inflammatory cytokines and COX-2 in cultured human microglia. J Neuroimmunol 2005;159:66–74
18. Choi HB, Hong SH, Ryu JK, et al. Differential activation of subtype purinergic receptors modulates Ca^{2+} mobilization and COX-2 in human microglia. Glia 2003;43:95–103
19. Walker DG, Beach TG, Xu R, et al. Expression of the proto-oncogene Ret, a component of the GDNF receptor complex, persists in human substantia nigra neurons in Parkinson's disease. Brain Res 1998;792:207–17
20. Ryu JK, Franciosi S, Sattayaprasert P, et al. Minocycline inhibits neuronal death and glial activation induced by beta-amyloid peptide in rat hippocampus. Glia 2004;48:85–90
21. Faria RX, Defarias FP, Alves LA. Are second messengers crucial for opening the pore associated with $P2X_7$ receptor? Am J Physiol Cell Physiol 2005;288:C260–71
22. Di Virgilio F, Ferrari D, Falzoni S, et al. P2 purinoceptors in the immune system. Ciba Found Symp 1996;198:290–302, discussion 302–305
23. Inoue K. Microglial activation by purines and pyrimidines. Glia 2002; 40:156–63
24. Neary JT, Rathbone MP, Cattabeni F, et al. Trophic actions of extracellular nucleotides and nucleosides on glial and neuronal cells. Trends Neurosci 1996;19:13–18
25. Hirai K, Aliev G, Nunomura A, et al. Mitochondrial abnormalities in Alzheimer's disease. J Neurosci 2001;21:3017–23
26. Rampe D, Wang L, Ringheim GE. $P2X_7$ receptor modulation of beta-amyloid- and LPS-induced cytokine secretion from human macrophages and microglia. J Neuroimmunol 2004;147:56–61
27. Bulanova E, Budagian V, Orinska Z, et al. Extracellular ATP induces cytokine expression and apoptosis through $P2X_7$ receptor in murine mast cells. J Immunol 2005;174:3880–90
28. Ferrari D, Chiozzi P, Falzoni S, et al. ATP-mediated cytotoxicity in microglial cells. Neuropharmacology 1997;36:1295–301
29. Verderio C, Matteoli M. ATP mediates calcium signaling between astrocytes and microglial cells: Modulation by IFN-gamma. J Immunol 2001;166:6383–91
30. Narcisse L, Scemes E, Zhao Y, et al. The cytokine IL-1beta transiently enhances $P2X_7$ receptor expression and function in human astrocytes. Glia 2005;49:245–58
31. Di Virgilio F, Chiozzi P, Falzoni S, et al. Cytolytic P2X purinoceptors. Cell Death Differ 1998;5:191–99
32. Ferrari D, Pizzirani C, Adinolfi E, et al. The $P2X_7$ receptor: A key player in IL-1 processing and release. J Immunol 2006;176:3877–83
33. Duan S, Anderson CM, Keung EC, et al. $P2X_7$ receptor-mediated release of excitatory amino acids from astrocytes. J Neurosci 2003;23: 1320–28
34. Gu BJ, Wiley JS. Rapid ATP-induced release of matrix metalloproteinase 9 is mediated by the $P2X_7$ receptor. Blood 2006;107: 4946–53
35. Akiyama H, Barger S, Barnum S, et al. Inflammation and Alzheimer's disease. Neurobiol Aging 2000;21:383–421
36. Walker DG, Link J, Lue LF, et al. Gene expression changes by amyloid beta peptide-stimulated human postmortem brain microglia identify activation of multiple inflammatory processes. J Leukoc Biol 2006;79: 596–610

